Supporting Information

Ultralong Room-Temperature Phosphorescence Remarkably Weakened by Halogenation-Induced Molecular Packing in Hexaphenylmelamine Derivatives

Qiang Guo,[a] Shiyi Zhou,[a] Xiaoyu Li,[b] Li Tao,[a] Mengke Li,[c] Shi-Jian Su,[c] Danyang Wan,[d] and Jie Li *[a]

[a] *College of Optoelectronic Engineering, Chengdu University of Information Technology, Chengdu 610225, China.*

[b] *Southwest University of Science and Technology, Mianyang 621010, China*

[c] *State Key Laboratory of Luminescent Materials and Devices and Institute of Polymer Optoelectronic Materials and Devices, South China University of Technology, Guangzhou 510640, China*

[d] *Optical and Electrical Material Center, Xi'an Modern Chemistry Research Institute, Xi'an 710065, China*

** E-mail: lijie@cuit.edu.cn*

Table of Contents

I. General remarks

1. Materials

Unless otherwise noted, diphenylamine, 4-chloro-*N*-phenylaniline, 4-bromo-*N*-phenylaniline, cyanuric chloride, n-BuLi (2.5 M in hexane), lithium diisopropylamide (LDA, 2 M in THF) and extra dry solvents (THF stored with molecular sieves) were obtained from commercial suppliers and used without further purification. 4-Fluoro-*N*-phenylaniline [S1] and 2-chloro-4,6-bis(diphenylamino)-1,3,5-trazine [S2] were prepared according to the literatures.

2. Instrumentation

NMR spectra were obtained on a Varian Inova 400 spectrometer. The ^{1}H NMR (400 MHz) and ^{13}C NMR (100 MHz) chemical shifts were measured relative to $CDCl_3$ as the internal reference ($CDCl_3$: δ = 7.26 ppm for ^{1}H and δ = 77.16 ppm for ^{13}C, respectively). High-resolution mass spectra (HRMS) were obtained with Waters-Q-TOF-Premier (ESI^+). The purities of **HPM** derivatives were determined by high-performance liquid chromatography (HPLC) using an Agilent 1260-DAD HPLC system. Single-crystal X-ray diffraction data for the compounds were obtained by using a New Gemini, Dual, Cu at zero, EosS2 diffractometer or a Bruker D8 venture diffractometer with Ga radiation at room temperature. Using Olex2 [S3], the structure was solved with the ShelXT [S4] structure solution program using Intrinsic Phasing and refined with the ShelXL [S5] refinement package using Least Squares minimisation. The UV-vis diffuse reflectance spectra (DRS) were obtained by SHIMADZU UV-3600 plus equipped with integrating sphere attachment. Room-temperature phosphorescence (RTP) spectra were measured using HITACHI F-7100 FL spectrophotometer (phosphorescence mode, chopping speed: 40 Hz). The RTP lifetimes were collected on a HORIBA TEMPRO-01 instrument. The phosphorescence quantum yields were determined by FLS-980 with integrating sphere systems under ambient conditions. The time-resolved RTP decay image and temperature dependent phosphorescence spectra were obtained by FLS-980. The lifetimes of temperature dependence of phosphorescence were recorded by the QM-40 spectrofluorometer employing an electric shutter, and the excitation source is a nitrogen laser (λ = 337 nm, pulse width $\approx$ 1.5 ns, repetition rate = 11 Hz). 10 K was obtained by cycle refrigeration of liquid helium using ARS-4HW cryo equipment (Advanced Research Systems). Powder X-ray diffraction (PXRD) patterns for **HPM** derivatives were recorded from 5.0° to 50.0° (2θ) using a Dandong DX-2700 powder diffractometer equipped with a copper target X-ray tube and a diffracted beam monochromator. Differential scanning calorimetry (DSC) analysis were measured by Mettler Toledo DSC1 under nitrogen atmosphere at heating and cooling rate of 5 °C/min.

II. Synthesis procedures

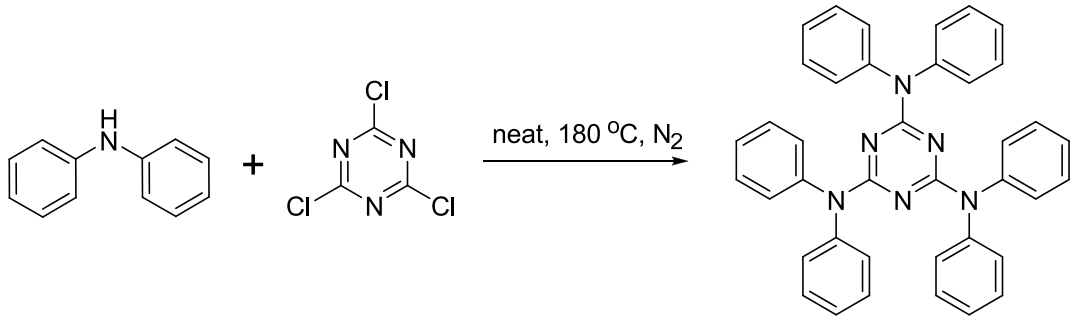

Scheme S1 Synthesis of **HPM-H**.

2,4,6-Tris(diphenylamino)-1,3,5-triazine (HPM-H): HPM-H was synthesized according to the literature and recrystallized from DMF [S6]. ^{1}H NMR (400 MHz, $CDCl_3$): δ = 7.11-7.15 (m, 24 H), 7.01-7.06 (m, 6H) ppm. ^{13}C NMR (100 MHz, $CDCl_3$): δ = 165.8, 143.6, 128.4, 127.6, 125.0 ppm. Purity: 99.90% (HPLC).

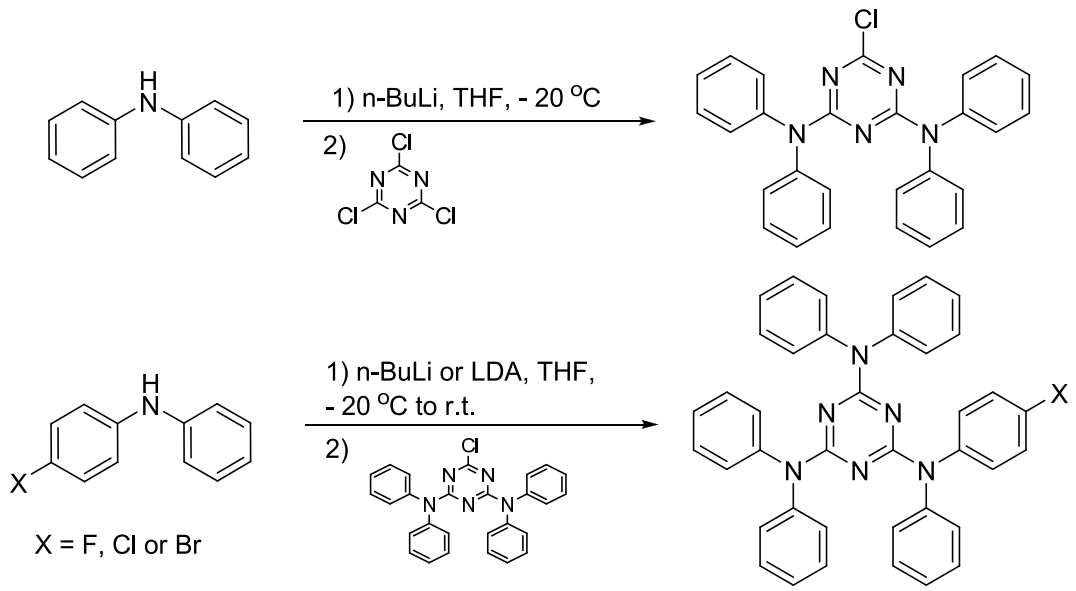

Scheme S2 Synthesis of **HPM-F**, **HPM-Cl** and **HPM-Br**.

2-[*N*,*N*-(4-fluorophenyl)phenylamino)]-4,6-bis(diphenylamino)-1,3,5-trazine (HPM-F): 4-Fluoro-*N*-phenylaniline (374.4 mg, 2 mmol) and 10 mL dry THF were palced in a flame-dried Schlenk tube with a magnetic stir bar under a N_2 atmosphere. Then the solution was cooled to -20 °C and *n*-BuLi (2.5 M in hexane, 0.96 mL, 2.4 mmol) was dropped slowly into the solution. The mixture was then warmed to room temperature and 2-chloro-4,6-bis(diphenylamino)-1,3,5-trazine (899.9 mg, 2 mmol) was added. The mixture was heated at 80 °C overnight. A large amount of solid product was precipitated. The precipitation was filtered and washed with

methanol several times. The desired product was then recrystallized from xylene and dried in vacuo to give a white solid (722 mg, 60%). ^{1}H NMR (400 MHz, $CDCl_3$): δ = 7.10-7.16 (m, 20 H), 7.03-7.07 (m, 7H), 6.76-6.82 (m, 2H) ppm. ^{13}C NMR (100 MHz, $CDCl_3$): δ = 165.8, 165.7, 161.4, 158.9, 143.5, 143.3, 139.54, 139.51, 129.4, 129.3, 128.39, 128.36, 127.6, 127.3, 125.1, 125.0, 115.2, 115.0 ppm. HRMS (ESI^+): calcd. for $C_{39}H_{30}FN_6$ $[M+H]^+$ 601.2516, found 601.2516. Purity: 99.32% (HPLC).

2-[*N,N*-(4-chlorophenyl)phenylamino)]-4,6-bis(diphenylamino)-1,3,5-trazine (HPM-Cl): 4-Chloro-*N*-phenylaniline (672.1 mg, 3.3 mmol) and 15 mL dry THF were palced in a flame-dried Schlenk tube with a magnetic stir bar under a N_2 atmosphere. Then the solution was cooled to -20 °C and LDA (2 M in THF, 1.82 mL, 3.63 mmol) was dropped slowly into the solution. The mixture was then warmed to room temperature and 2-chloro-4,6-bis(diphenylamino)-1,3,5-trazine (1.35 g, 3 mmol) was added. The mixture was heated at 80 °C overnight. A large amount of solid product was precipitated. The precipitation was filtered and washed with methanol several times. The desired product was then recrystallized from xylene and dried in vacuo to give a white solid (1.02 g, 55%). ^{1}H NMR (400 MHz, $CDCl_3$): δ = 7.18-7.11 (m, 20 H), 7.09-7.01 (m, 9H) ppm. ^{13}C NMR (100 MHz, $CDCl_3$): δ = 165.8, 165.6, 143.5, 143.0, 142.1, 130.3, 128.8, 128.46, 128.41, 128.35, 127.6, 127.5, 125.23, 125.19 ppm. HRMS (ESI^+): calcd. for $C_{39}H_{30}ClN_6$ $[M+H]^+$ 617.2220, found 617.2200. Purity: 99.58% (HPLC).

2-[*N,N*-(4-bromophenyl)phenylamino)]-4,6-bis(diphenylamino)-1,3,5-trazine (HPM-Br): 4-Bromo-*N*-phenylaniline (545.9 mg, 2.2 mmol) and 10 mL dry THF were palced in a flame-dried Schlenk tube with a magnetic stir bar under a N_2 atmosphere. Then the solution was cooled to -20 °C and LDA (2 M in THF, 132 mL, 2.64 mmol) was dropped slowly into the solution. The mixture was then warmed to room temperature and 2-chloro-4,6-bis(diphenylamino)-1,3,5-trazine (899.9 g, 2.0 mmol) was added. The mixture was heated at 80 °C overnight. A large amount of solid product was precipitated. The precipitation was filtered and washed with methanol several times. The desired product was then recrystallized from xylene and dried in vacuo to give a white solid (709 mg, 54%). ^{1}H NMR (400 MHz, $CDCl_3$): δ = 7.18-7.11 (m, 20 H), 7.09-7.01 (m, 9H) ppm. ^{13}C NMR (100 MHz, $CDCl_3$): δ = 165.8, 165.5, 143.4, 143.0, 142.7, 131.3, 129.1, 128.47, 128.42, 127.6, 127.5, 125.3, 125.2, 118.2 ppm. HRMS (ESI^+): calcd. for $C_{39}H_{30}BrN_6$ $[M+H]^+$ 661.1715, found 661.1716. Purity: 99.63% (HPLC).

III. Photophysical, XRD and DSC Properties

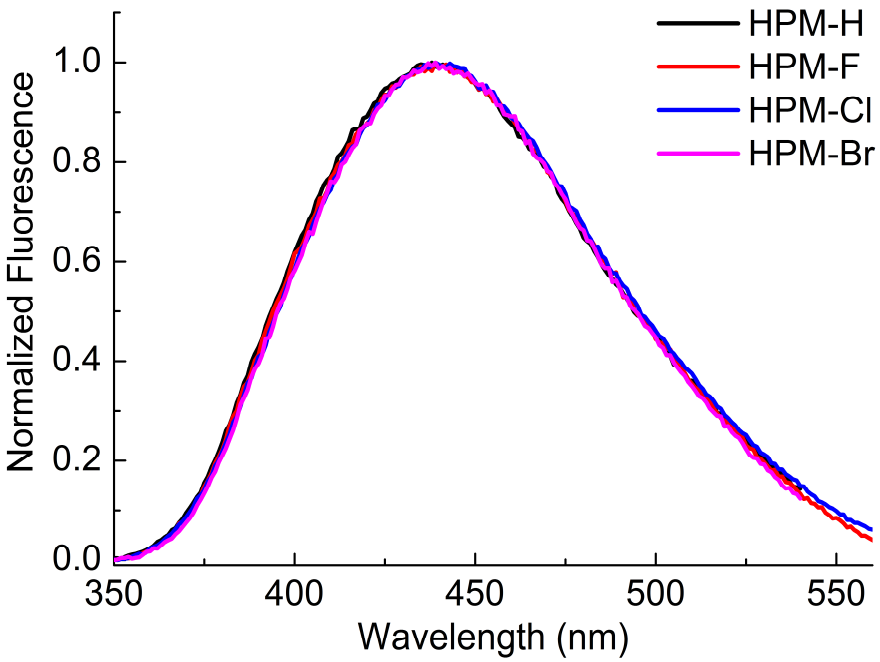

Fig. S1 The fluorescence spectra of **HPM** derivatives in diluted THF solution (2×10^{-5} mol/L) at 300 K.

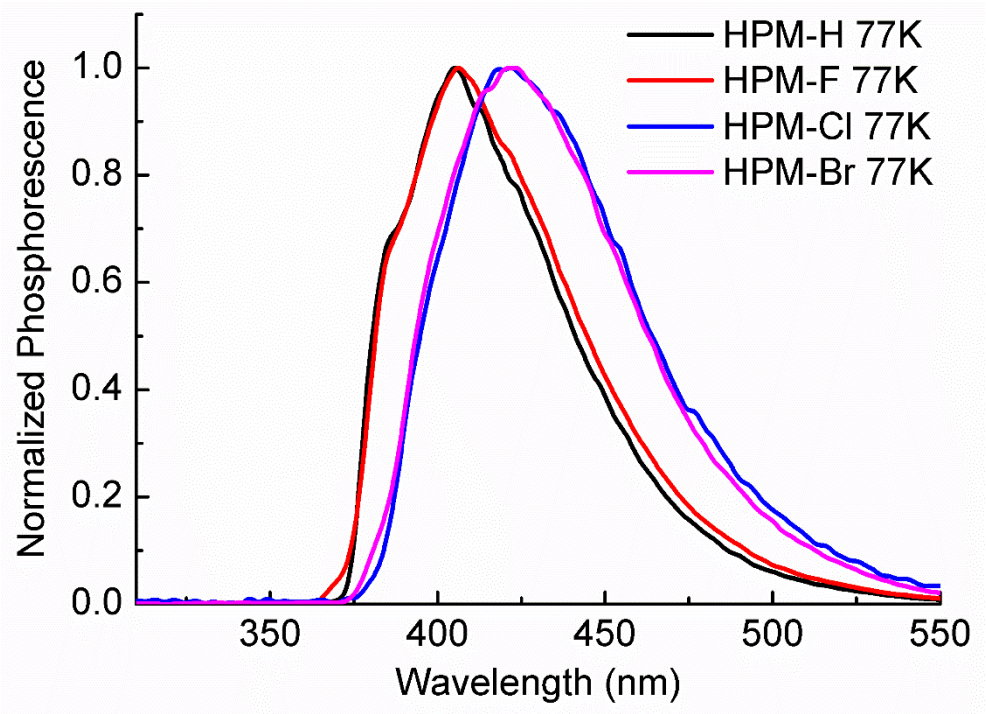

Fig. S2 The phosphorescence spectra of **HPM** derivatives in diluted THF solution (2×10^{-5} mol/L) at 77 K.

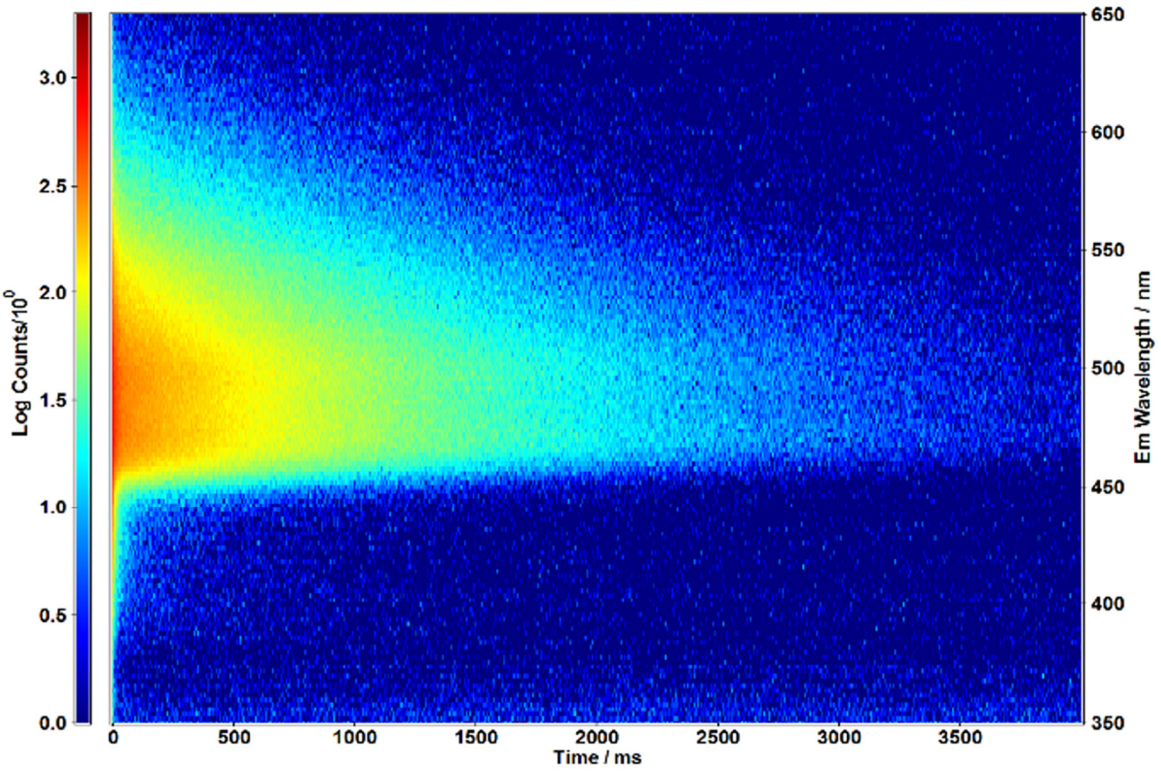

Fig. S3 The time-resolved RTP decay images of **HPM-H** in crystals.

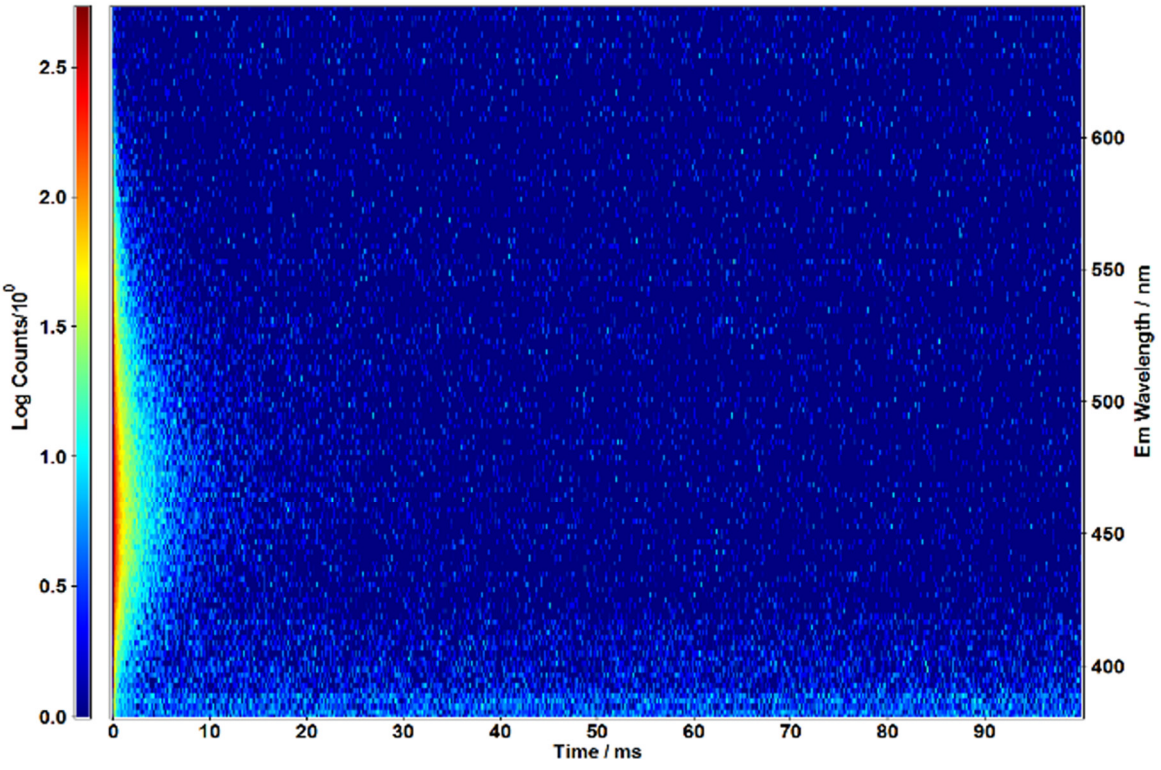

Fig. S4 The time-resolved RTP decay images of **HPM-Br** in crystals.

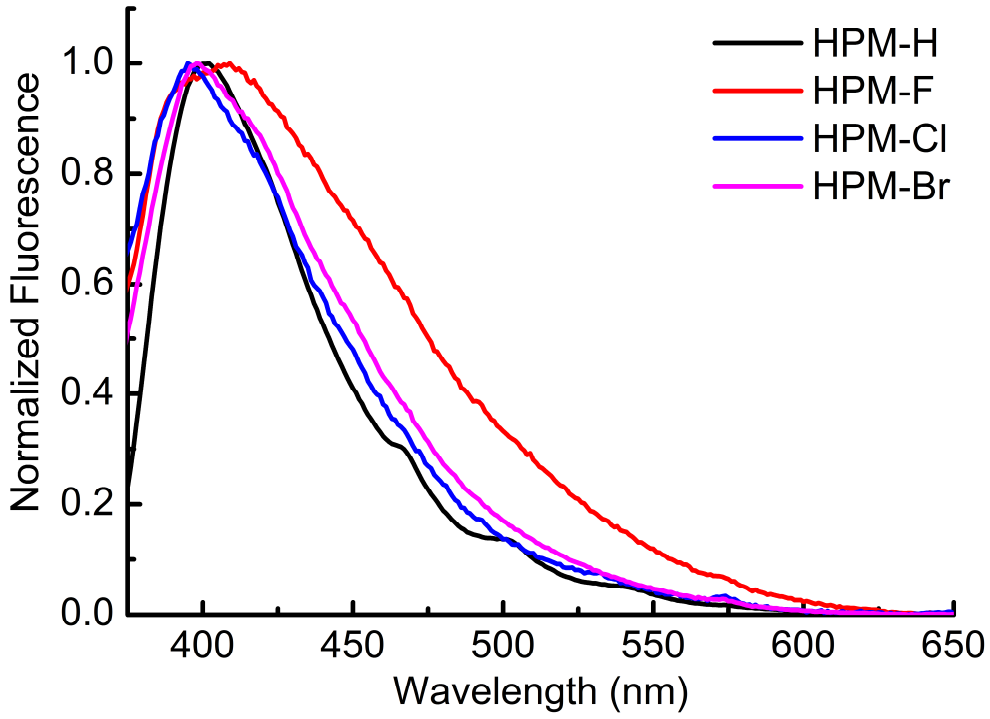

Fig. S5 The fluorescence spectra of **HPM** derivatives in crystals at 300 K.

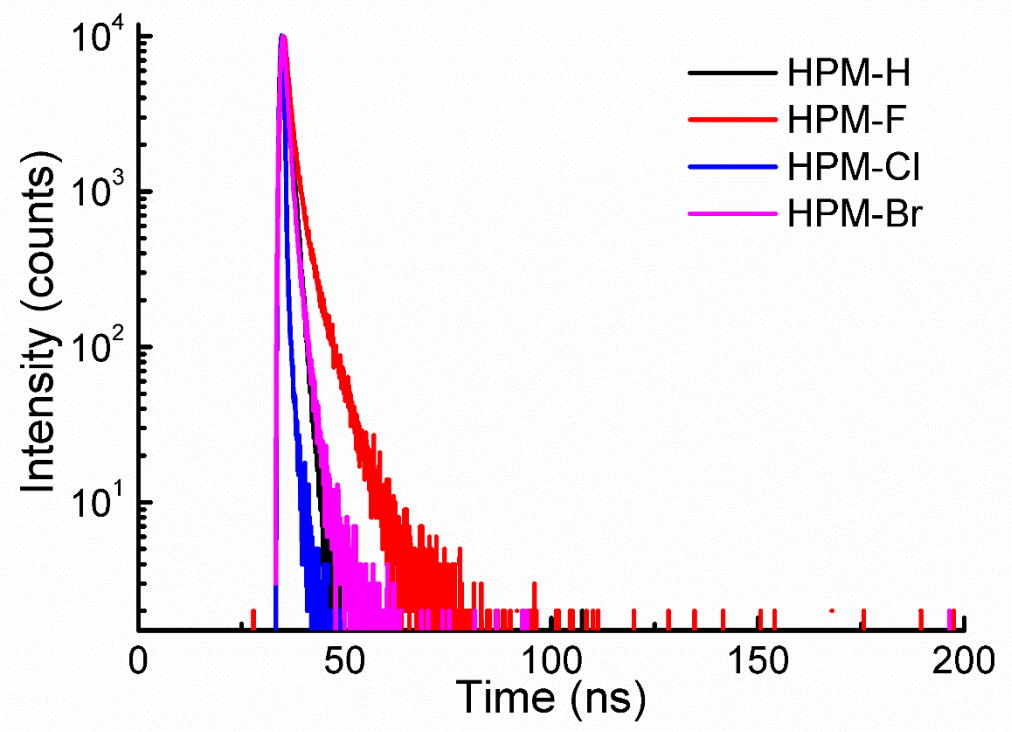

Fig. S6 The time-resolved PL decay curves of **HPM** derivatives in crystals at 300 K in the time range of 200 ns.

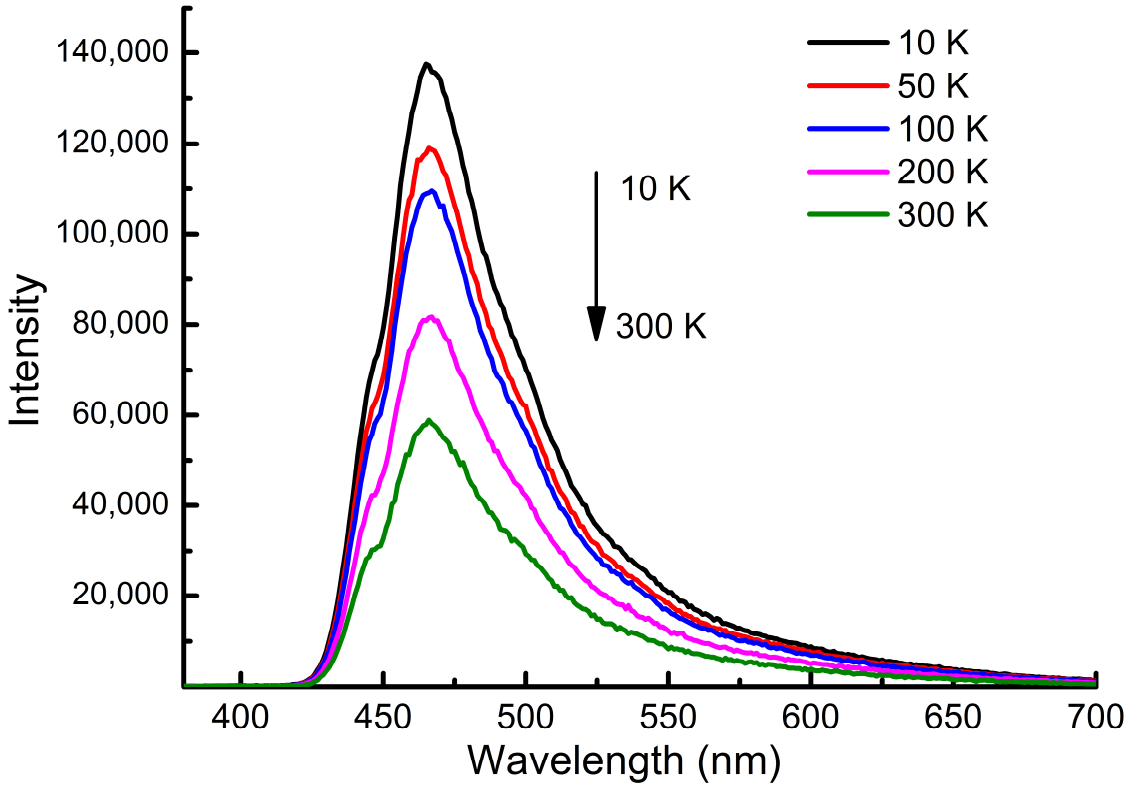

Fig. S7 The temperature dependent phosphorescence spectra for the delayed component of **HPM-H** in crystals.

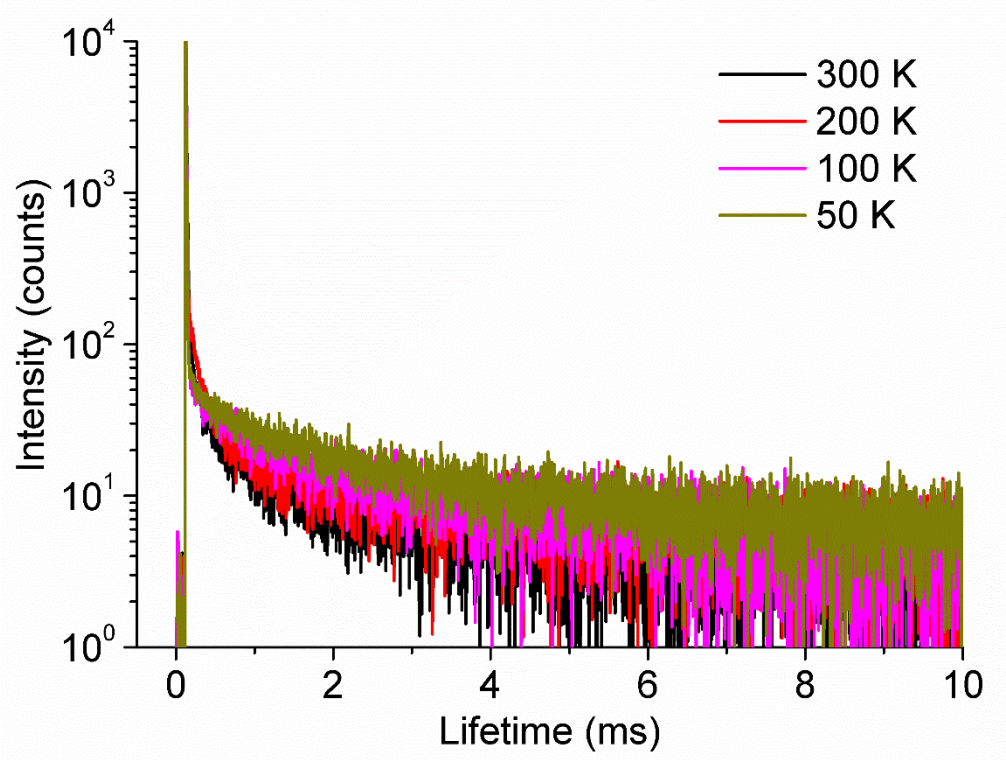

Fig. S8 The temperature dependence of time-resolved photoluminescence decay curves of **HPM-H** in crystals in the time range of 10 ms.

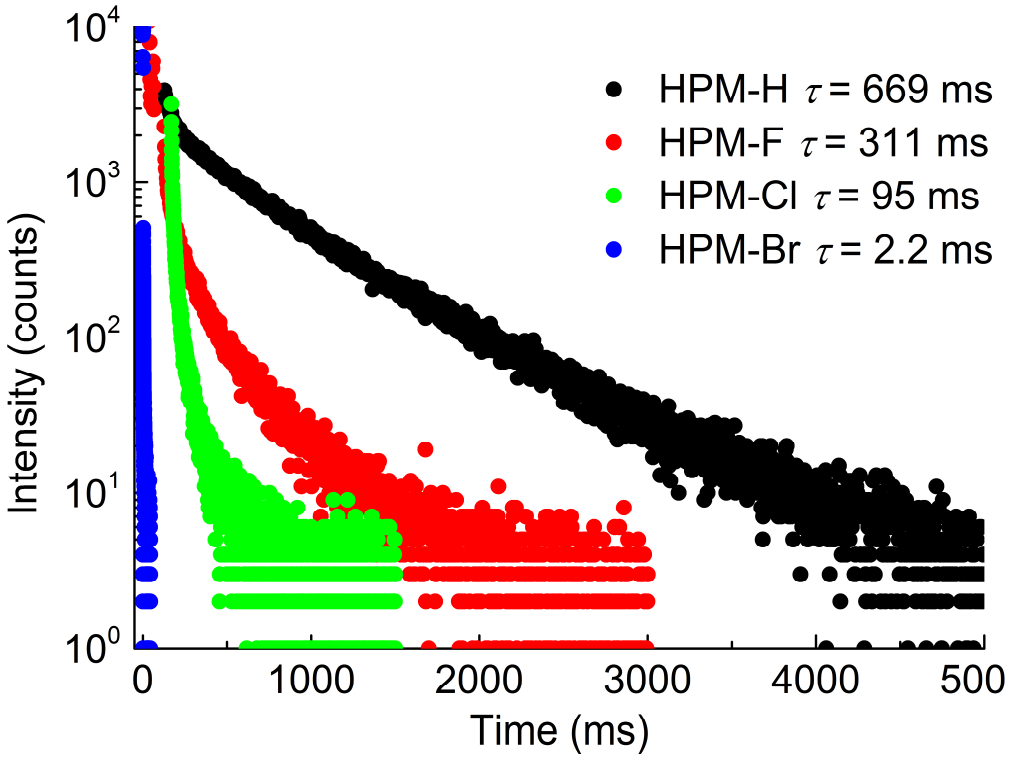

Fig. S9 The time-resolved RTP decay curves of shoulder emission peaks of **HPM** derivatives in crystals.

Table S1 The details of RTP lifetimes (τ) of **HPM** derivatives in crystals.

Compound	λ_{phos} (nm)	τ_1 (ms)	A_1 (%)	τ_2 (ms)	A_2 (%)
HPM-H	473	76.87	8.13	608.09	91.87
	494 (sh)	102.59	12.35	668.53	87.65
HPM-F	463 (sh)	45.73	34.92	311.47	65.08
	507	53.10	15.03	337.44	84.97
HPM-Cl	501 (sh)	11.86	52.03	94.68	47.97
	534	19.95	40.71	99.32	59.29
HPM-Br	502 (sh)	0.38	26.98	2.23	73.02
	534	0.28	6.63	2.80	93.37

The lifetimes of shoulder emission peaks are quite similar to that of maximum emission peaks, indicating that all the photons are generated from the same excited state.

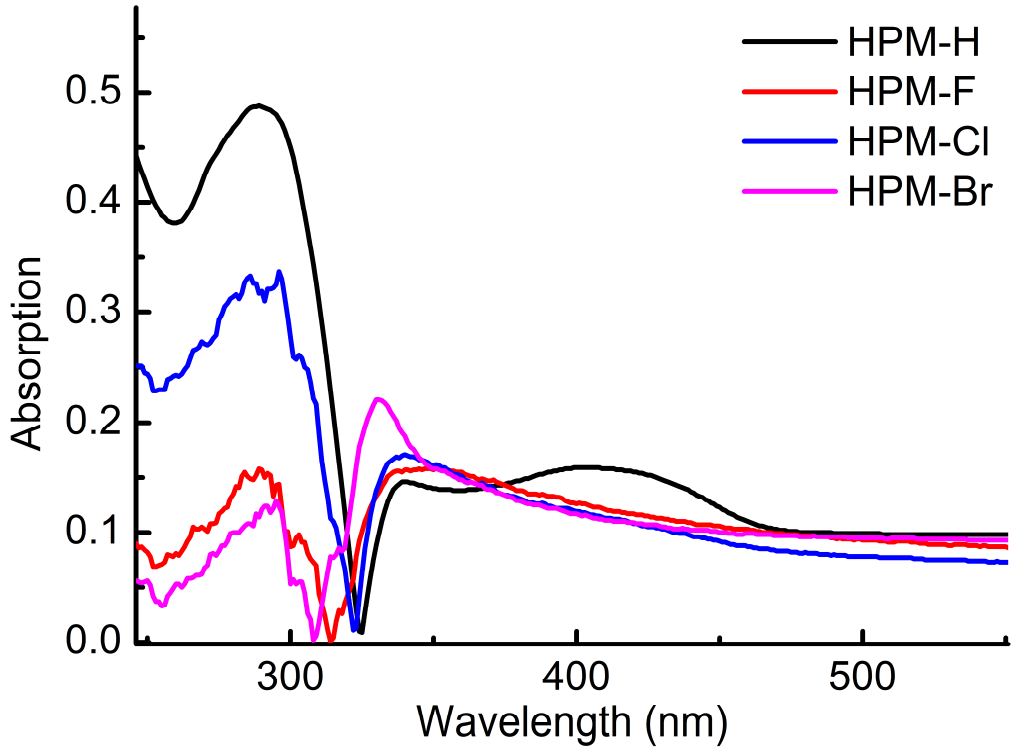

Fig. S10 The UV-vis DRS of **HPM** derivatives in powders.

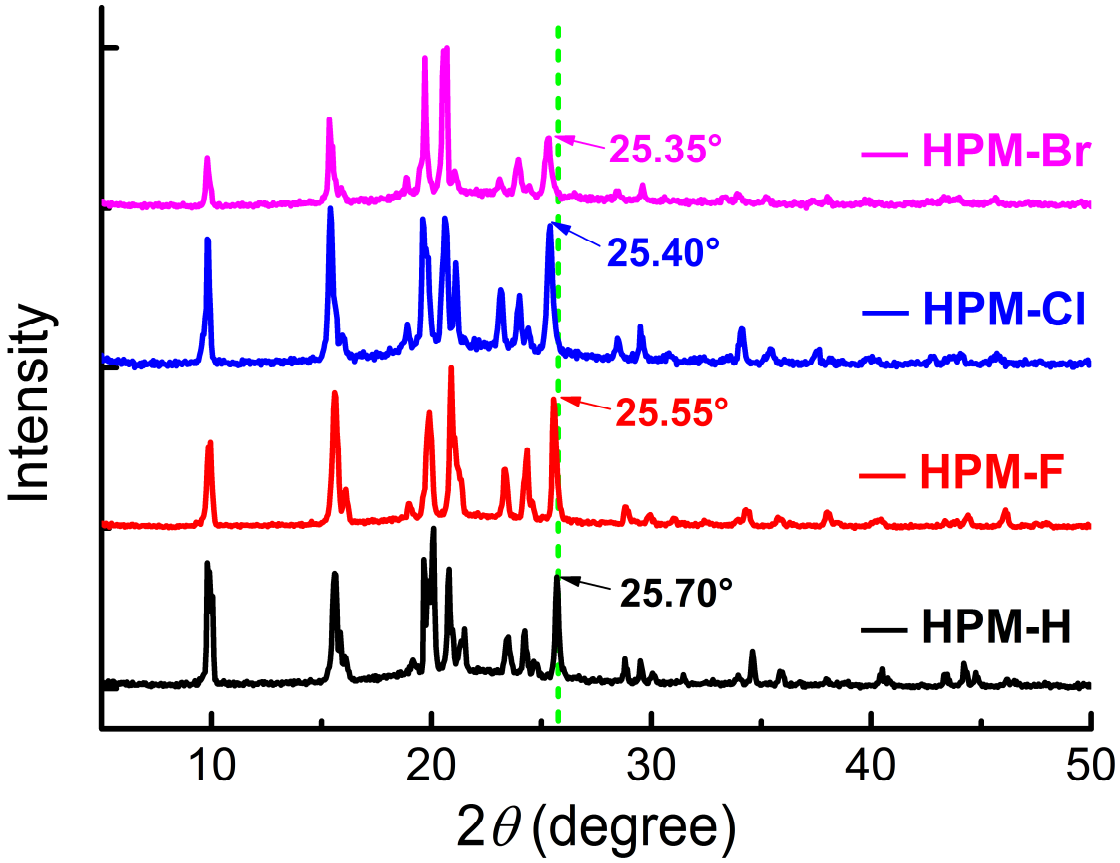

Fig. S11 The PXRD patterns of **HPM** derivatives.

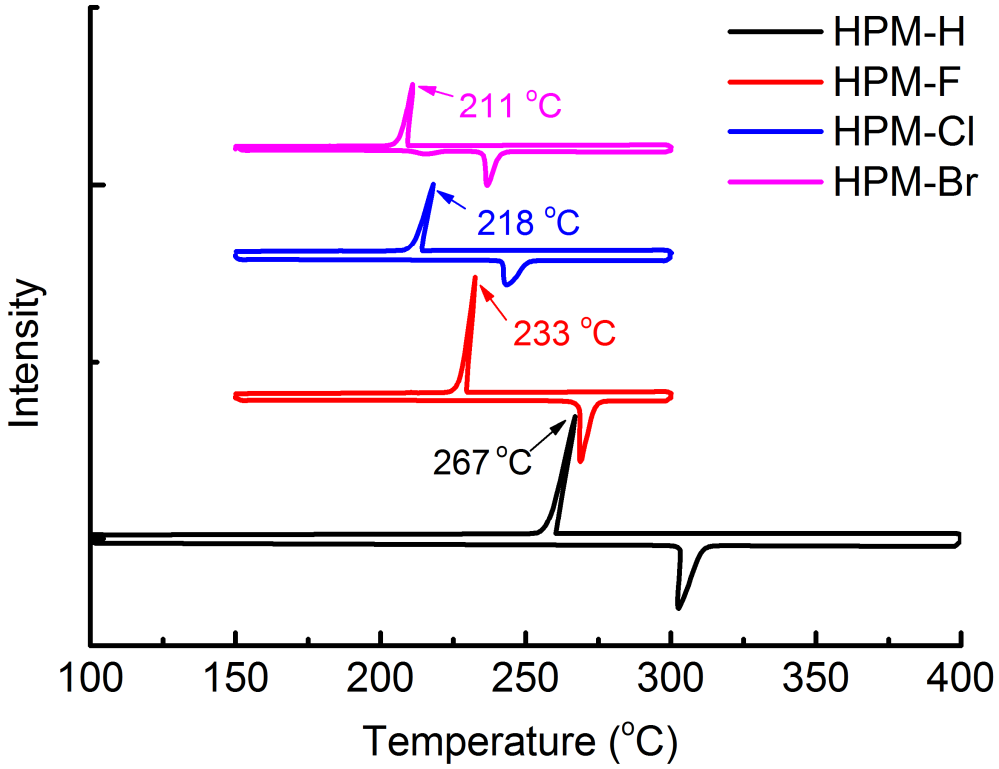

Fig. S12 The DSC curves of **HPM** derivatives.

Table S2 Single crystal data of **HPM** derivatives

Name	**HPM-H**	**HPM-F**	**HPM-Cl**	**HPM-Br**
Formula	$C_{39}H_{30}N_6$	$C_{39}H_{29}FN_6$	$C_{39}H_{29}ClN_6$	$C_{39}H_{29}BrN_6$
Wavelength (Å)	1.54184	1.54184	1.54184	1.34139
Space Group	R-3c	R-3c	R-3c	R-3c
Cell Lengths (Å)	a=14.4042(7) b=14.4042(7) c= 25.6105(13)	a=14.5389(9) b=14.5389(9) c=25.5523(16)	a=14.6313(7) b=14.6313(7) c=25.8672(16)	a=14.6985(7) b=14.6985(7) c=26.0926(13)
Cell Angles (°)	α =90 β =90 γ =120	α =90 β =90 γ =120	α =90 β =90 γ =120	α =90 β =90 γ =120
Cell Volume ($Å^3$)	4601.8(5)	4677.6(6)	4795.6(5)	4882.0(5)
Z	6	6	6	6
Density (g/cm^3)	1.262	1.279	1.282	1.350
F(000)	1836.0	1884.0	1932.0	2040.0
h_{max}, k_{max}, l_{max}	14,16,28	14,14,30	17,15,31	17,17,31
CCDC number	2063811	2063809	2063802	2063796

V. Theoretical calculations

The theoretical calculations were carried out by using Gaussian 16 A.03 package [S7]. To calculate the S_0 and T_1 geometries of structures in solid sates, the QM/MM method with two-layer ONIOM approach based on the single-crystal data were performed. The central molecule is regarded as high layer, calculated by QM method (B3LYP/6-31G* level). Meanwhile the surrounding molecules are frozen and regarded as low layer and calculated by MM method (UFF, embed QEq charge). The basis set superposition error (BSSE) corrected complexation energies (ΔE_c) of trimers of **HPM** derivatives were calculated to estimate the strength of noncovalent intermolecular interactions with functional and basis set of B3LYP-D3(BJ)/6-311+G(d,p). The molecular coordinates of **HPM** trimers were obtained from the single-crystal data, while the hydrogen and halogen atoms were optimized with B3LYP-D3(BJ)/6-311G(d,p) method. The geometry changes between S_0 and T_1 states are measured by root-mean squared displacement (RMSD) with the expression of $\mathrm{RMSD}=\sqrt{\frac{1}{N}\sum^{natom}\left[(x_i-x_i^{'})^2+(y_i-y_i^{'})^2+(z_i-z_i^{'})^2\right]}$.

The reorganization energy (ΔE_r) was calculated by MOMAP program [S8] to measure the non-radiative energy consumption based on the obtained electronic structure and vibration information. The total volume (V_{total}), free volume (V_{free}) were calculated by Multiwfn 3.8 based on the single-crystal unit cells data.

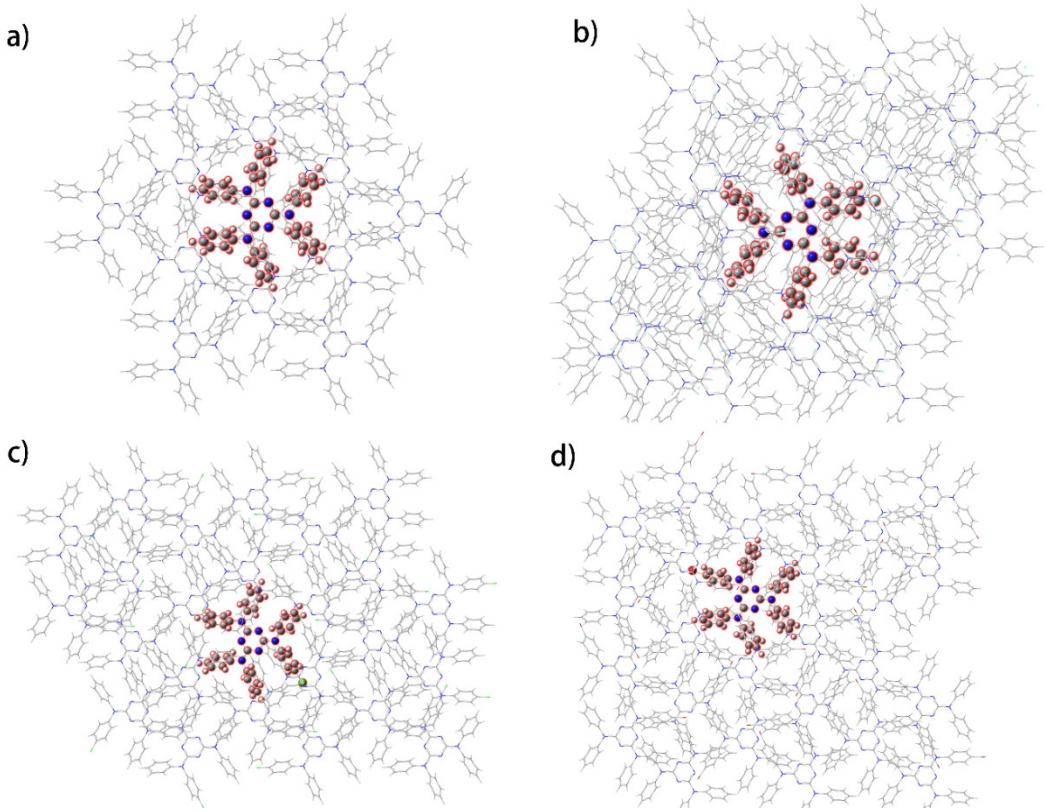

Fig. S13 QM/MM model for crystal (a) **HPM-H**, (b) **HPM-F**, (c) **HPM-Cl** and (d) **HPM-Br**, respectively.

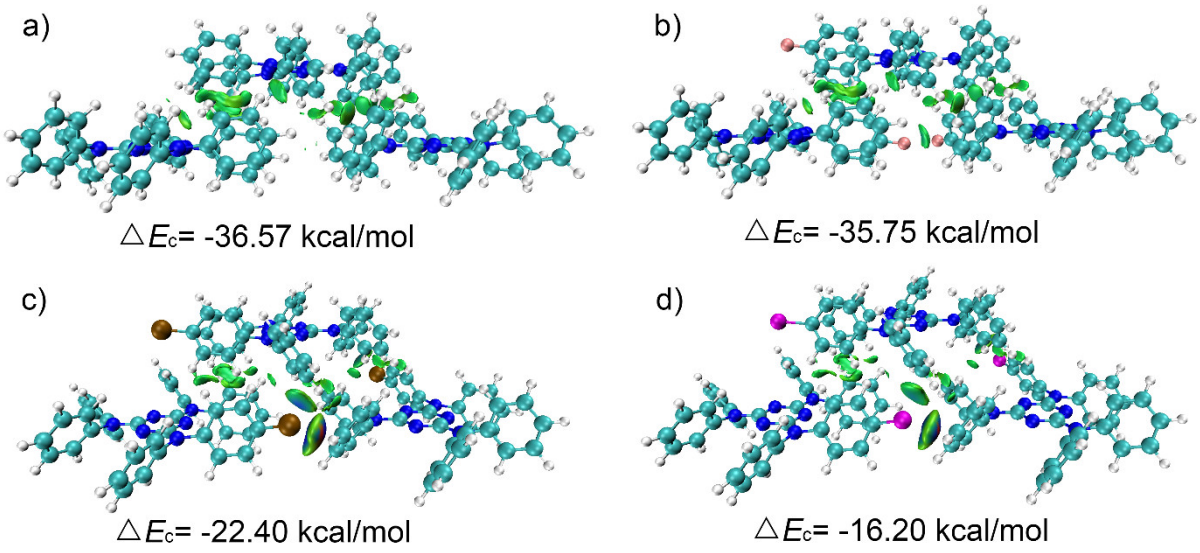

Fig. S14 Independent gradient model (IGM) gradient isosurface [S9-S11] and BSSE corrected complexation energies of **HPM** trimers, (a) **HPM-H**, (b) **HPM-F**, (c) **HPM-Cl** and (d) **HPM-Br**.

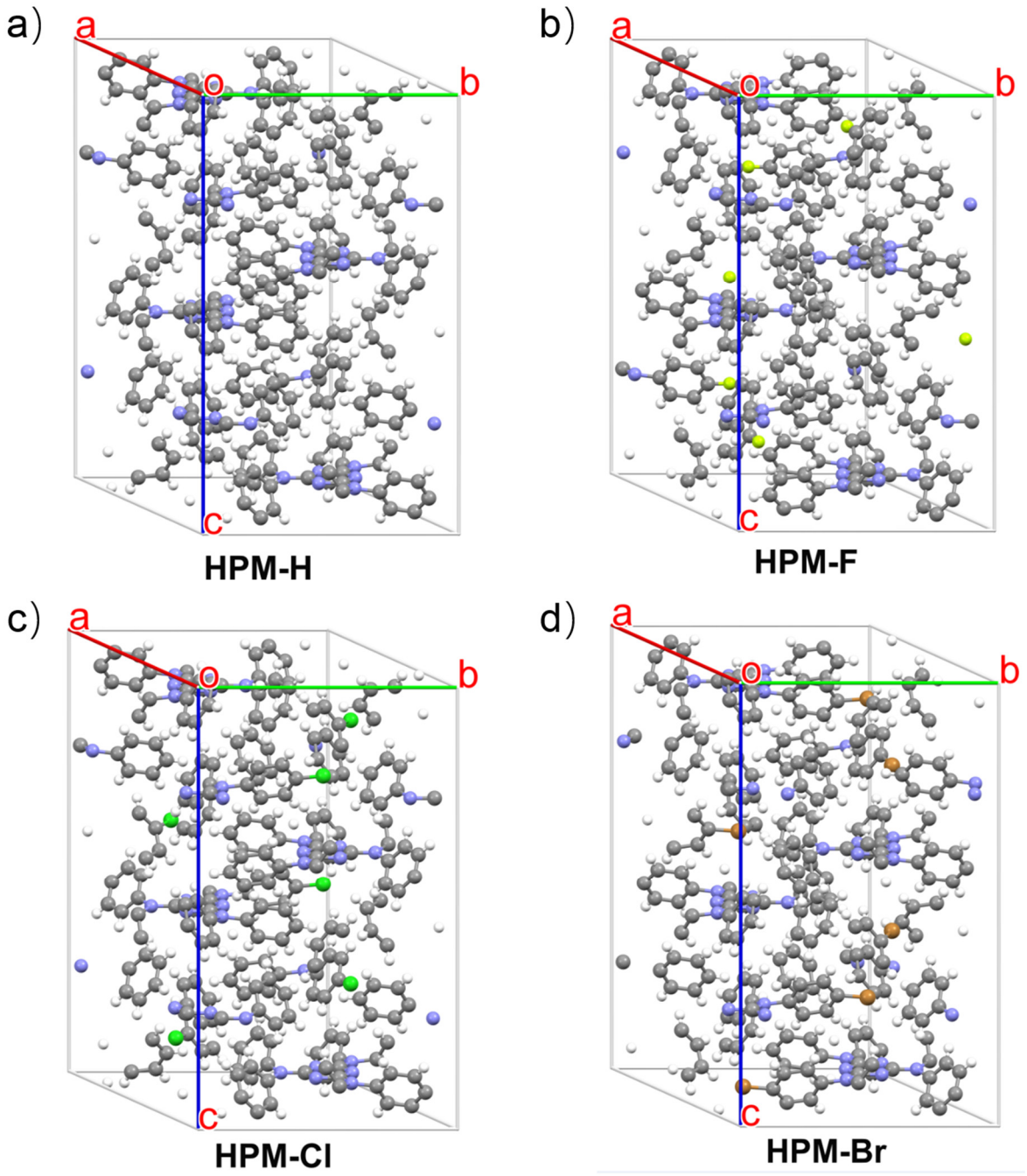

Fig. S15 Single-crystal unit cells of (a) **HPM-H**, (b) **HPM-F**, (c) **HPM-Cl** and (d) **HPM-Br**.

Table S3 Total volume (V_{total}), free volume (V_{free}) and V_{free}/V_{total} for single-crystal unit cells of **HPM** derivatives.

Compound	Total volume (V_{total}, Å^3)	Free volume (V_{free}, Å^3)	V_{free}/V_{total}
HPM-H	4601.85	1368.16	0.297306518
HPM-F	4677.66	1453.632	0.310760508
HPM-Cl	4795.65	1536.003	0.320290889
HPM-Br	4882.05	1597.24	0.327165842

V. References

[S1] J. Cao, J. R. Lever, T. Kopajtic, J. L. Katz, A. T. Pham, M. L. Holmes, J. B. Justice, A. H. Newman, *J. Med. Chem.* **2004**, *47*, 6128-6136.

[S2] Z-F. An, R.-F Chen, J. Yin, G.-H. Xie, H.-F. Shi, T. Tsuboi, W. Huang, *Chem. Eur. J.* **2011**, *17*, 10871-10878.

[S3] O. V Dolomanov, L. J. Bourhis, R. J. Gildea, J. A. K. Howard, H. Puschmann, *J. Appl. Cryst.* **2009**, *42*, 339-341.

[S4] G. M. Sheldrick, *Acta Cryst. A* **2015**, *71*, 3-8.

[S5] G. M. Sheldrick, *Acta Cryst. C* **2015**, *71*, 3-8.

[S6] F. León, P. Elizalde, P. Prieto, A. Sánchez-Migallón, *Dyes and Pigments*, **2016**, *131*, 307-319.

[S7] Gaussian 16, Revision A.03, M. J. Frisch, G. W. Trucks, H. B. Schlegel, G. E. Scuseria, M. A. Robb, J. R. Cheeseman, G. Scalmani, V. Barone, G. A. Petersson, H. Nakatsuji, X. Li, M. Caricato, A. V. Marenich, J. Bloino, B. G. Janesko, R. Gomperts, B. Mennucci, H. P. Hratchian, J. V. Ortiz, A. F. Izmaylov, J. L. Sonnenberg, D. Williams-Young, F. Ding, F. Lipparini, F. Egidi, J. Goings, B. Peng, A. Petrone, T. Henderson, D. Ranasinghe, V. G. Zakrzewski, J. Gao, N. Rega, G. Zheng, W. Liang, M. Hada, M. Ehara, K. Toyota, R. Fukuda, J. Hasegawa, M. Ishida, T. Nakajima, Y. Honda, O. Kitao, H. Nakai, T. Vreven, K. Throssell, J. A. Montgomery, Jr., J. E. Peralta, F. Ogliaro, M. J. Bearpark, J. J. Heyd, E. N. Brothers, K. N. Kudin, V. N. Staroverov, T. A. Keith, R. Kobayashi, J. Normand, K. Raghavachari, A. P. Rendell, J. C. Burant, S. S. Iyengar, J. Tomasi, M. Cossi, J. M. Millam, M. Klene, C. Adamo, R. Cammi, J. W. Ochterski, R. L. Martin, K. Morokuma, O. Farkas, J. B. Foresman, and D. J. Fox, Gaussian, Inc., Wallingford CT, **2016**.

[S8] MOMAP – Molecular Material Property Prediction Package. http://www.momap.net.cn

[S9] C. Lefebvre, G. Rubez, H. Khartabil, J.-C. Boisson, J. Contreras-García, E. Hénon, *Phys. Chem. Chem. Phys.* **2017**, *19*, 17928-17936.

[S10] T. Lu, F. Chen, *J. Comput. Chem.* **2012**, *33*, 580-592. Multiwfn 3.8 (dev) program: http://sobereva.com/multiwfn/ .

[S11] VMD 1.9.3 program: http://www.ks.uiuc.edu/Research/vmd/ .

VI. Copies of ^{1}H and ^{13}C NMR spectra of HPM derivatives

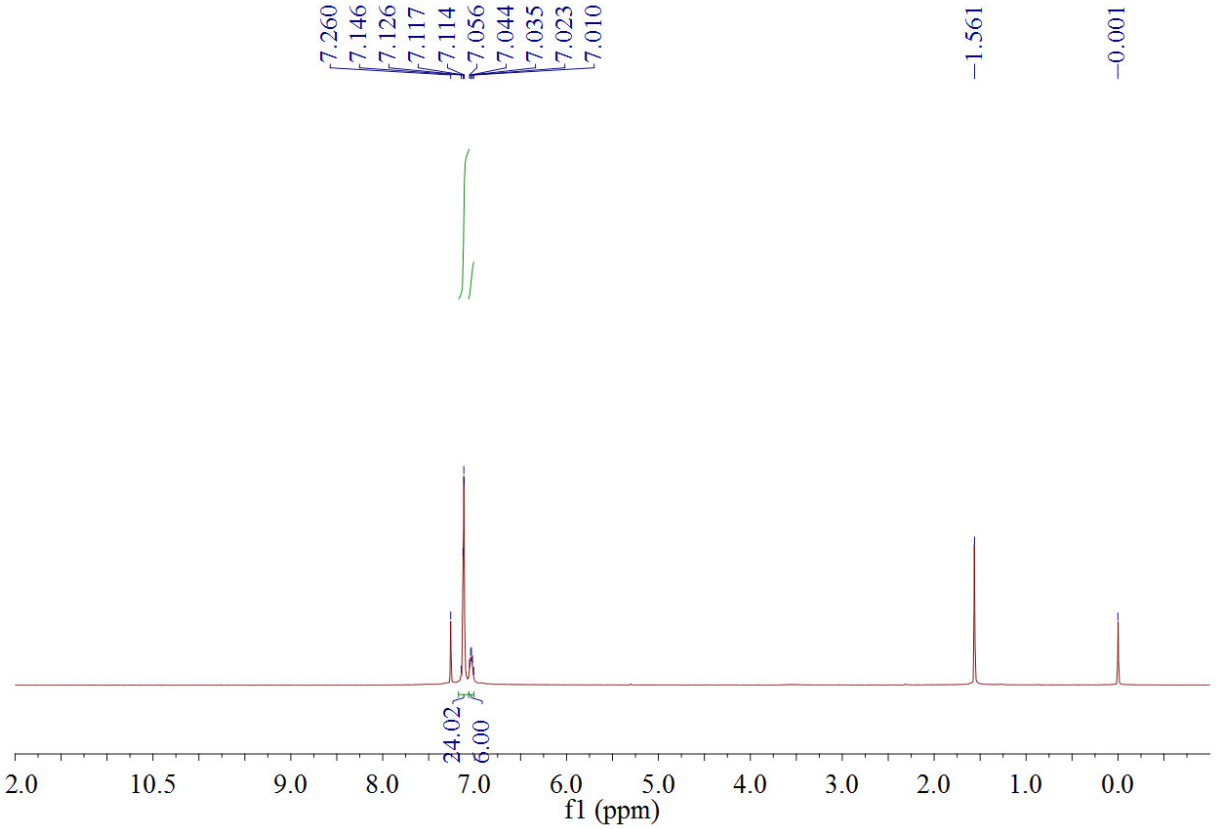

Fig. S16 ^{1}H NMR spectrum of **HPM-H** in $CDCl_3$.

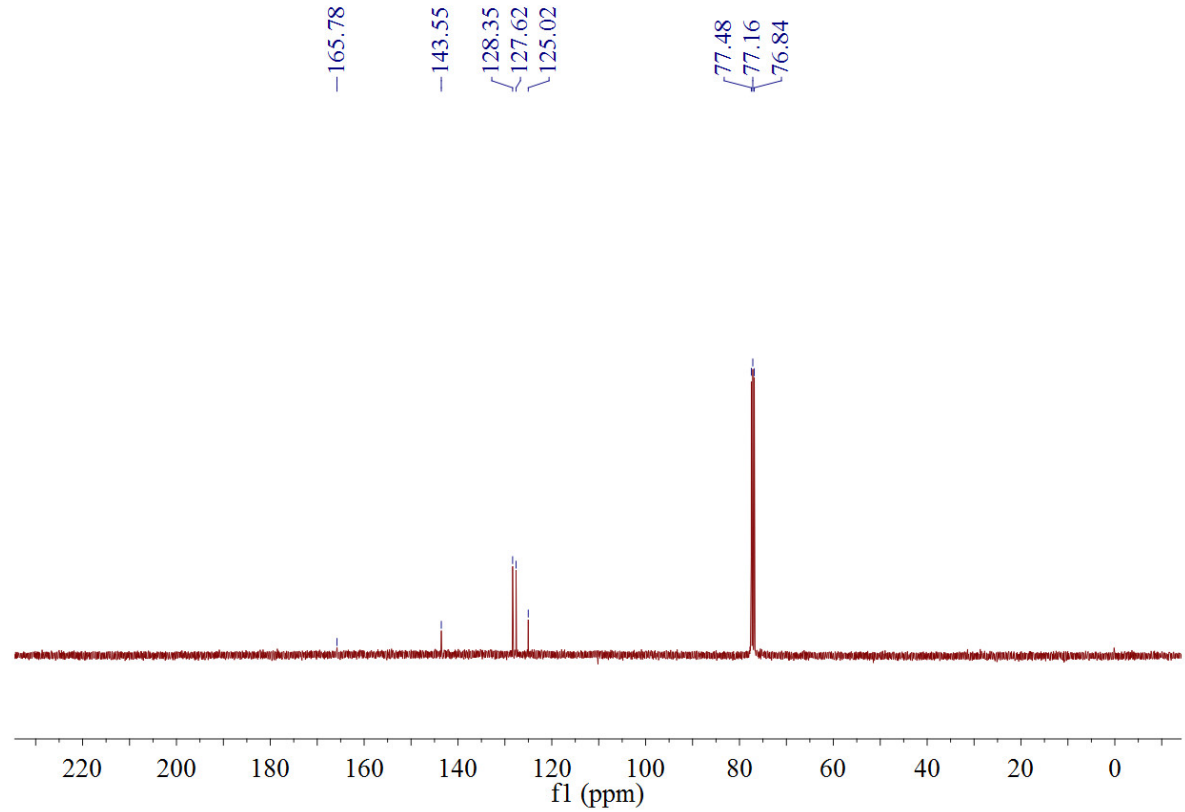

Fig. S17 ^{13}C NMR spectrum of **HPM-H** in $CDCl_3$.

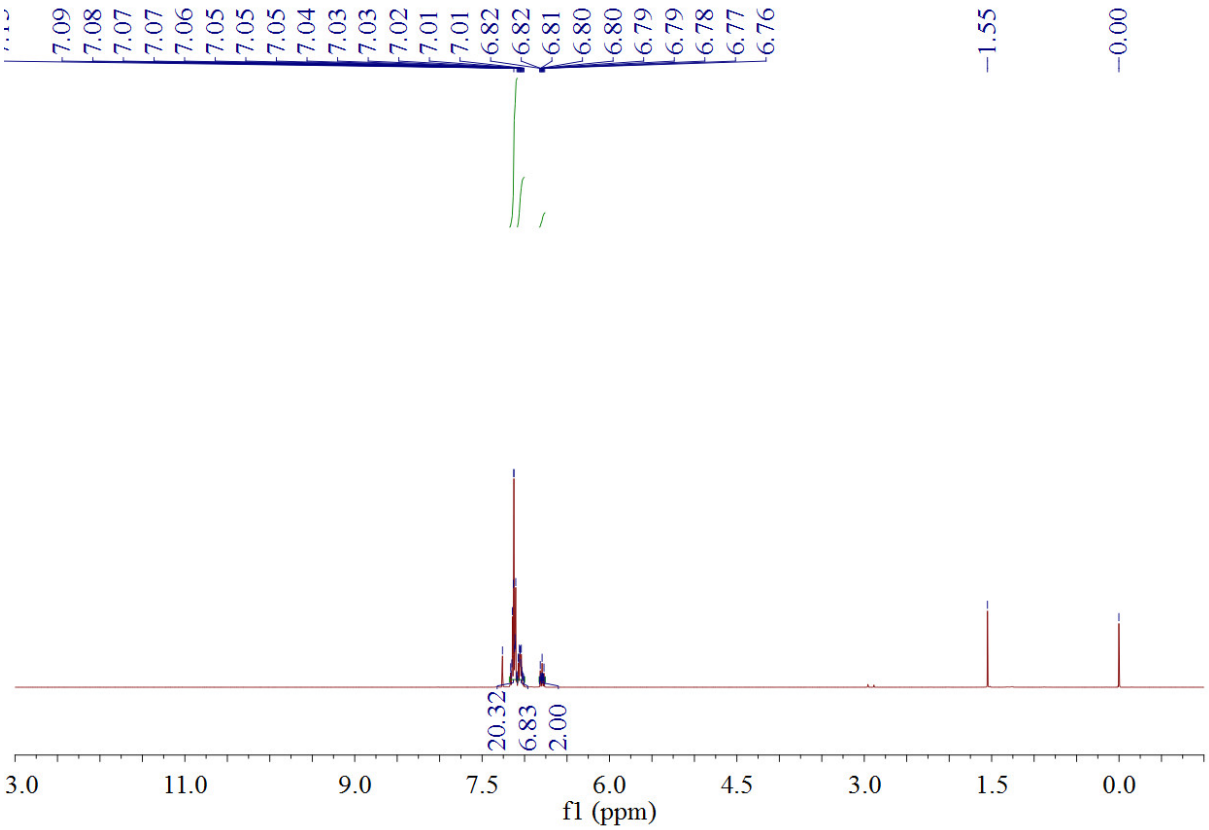

Fig. S18 ^{1}H NMR spectrum of **HPM-F** in $CDCl_3$.

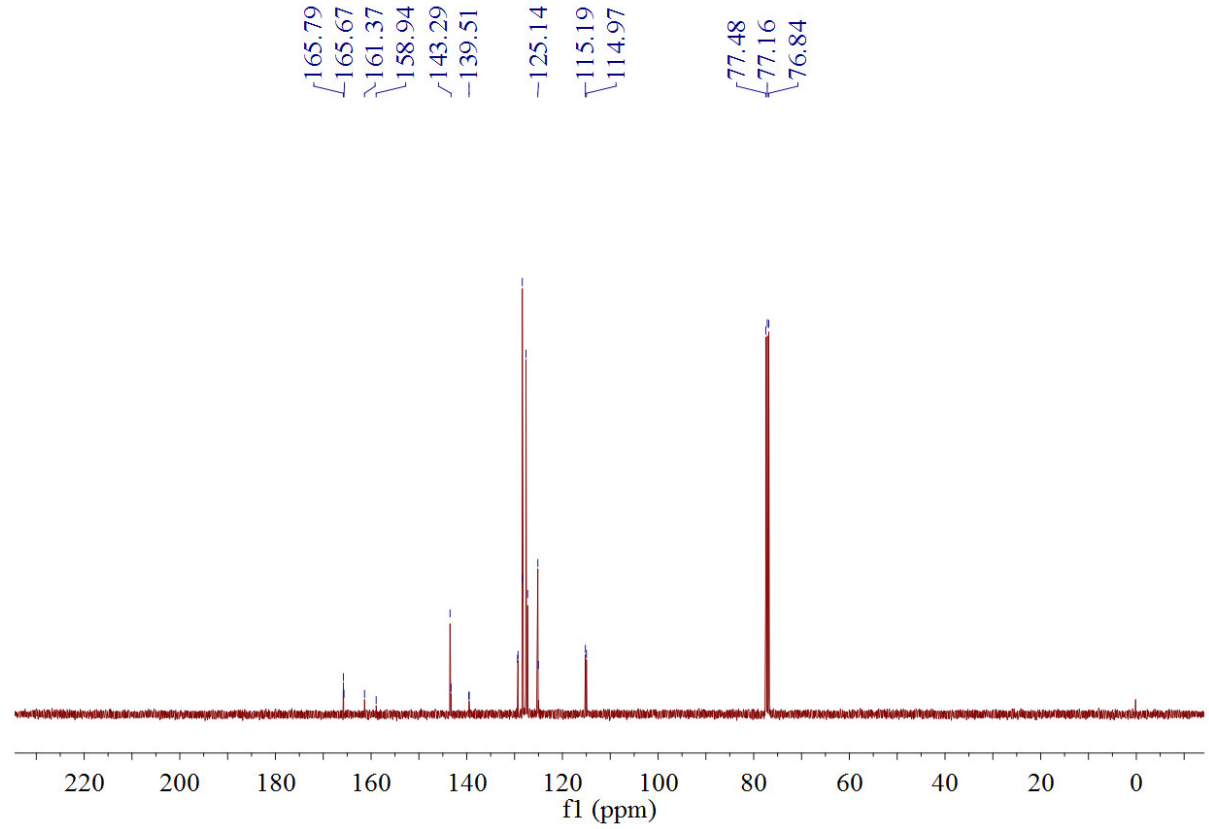

Fig. S19 ^{13}C NMR spectrum of **HPM-F** in $CDCl_3$.

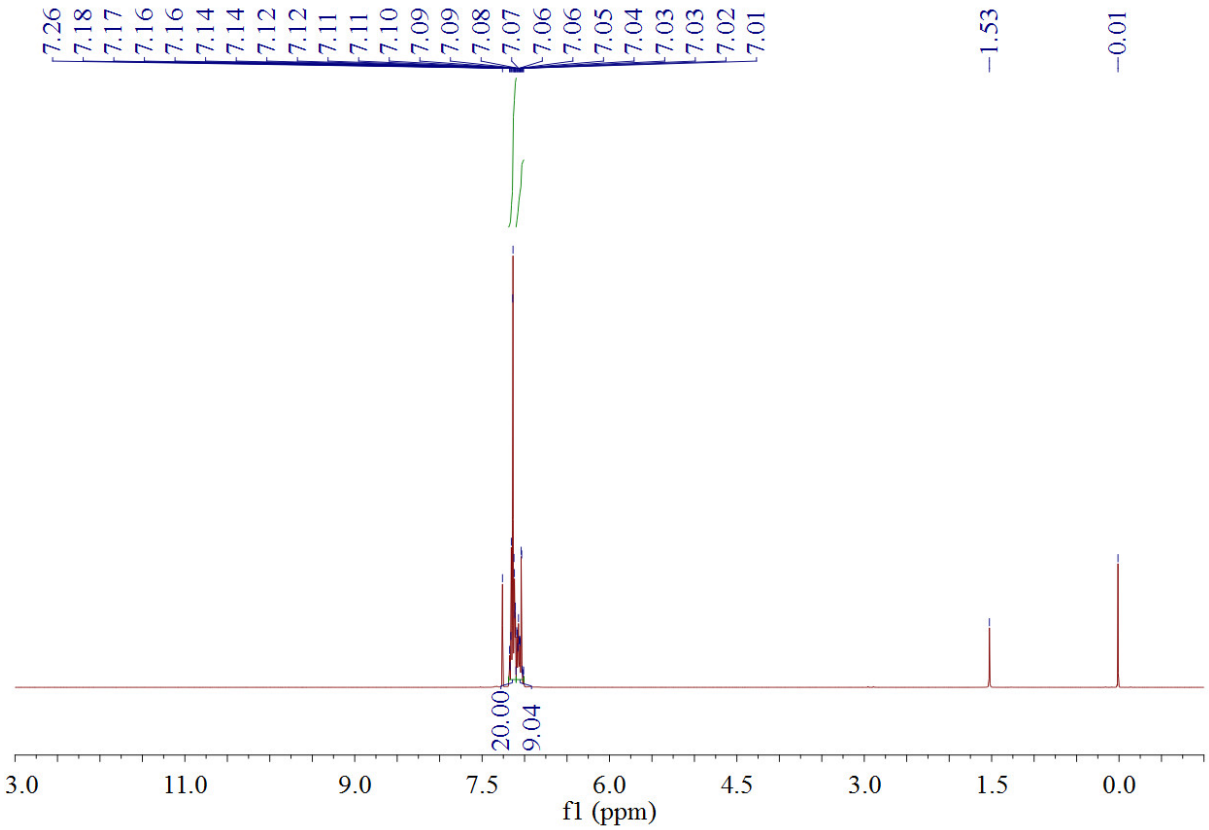

Fig. S20 ^{1}H NMR spectrum of **HPM-Cl** in $CDCl_3$.

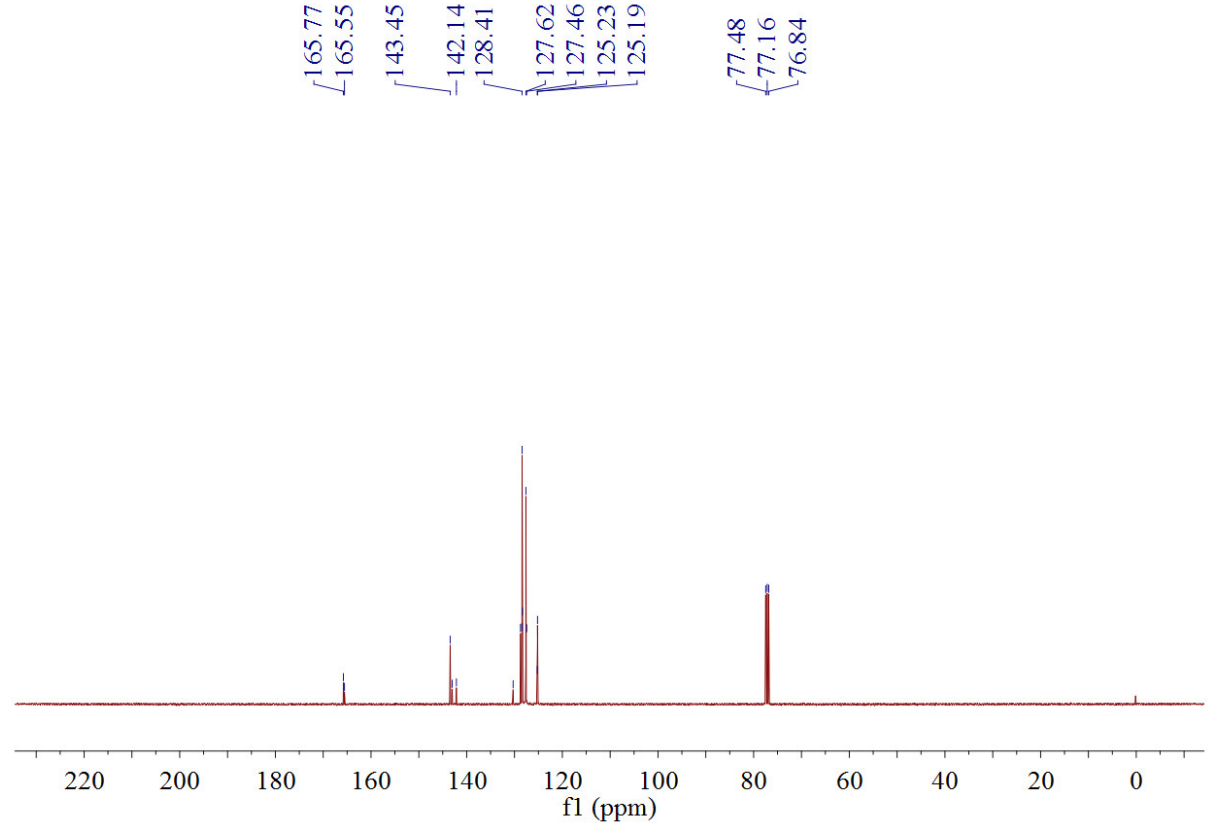

Fig. S21 ^{13}C NMR spectrum of **HPM-Cl** in $CDCl_3$.

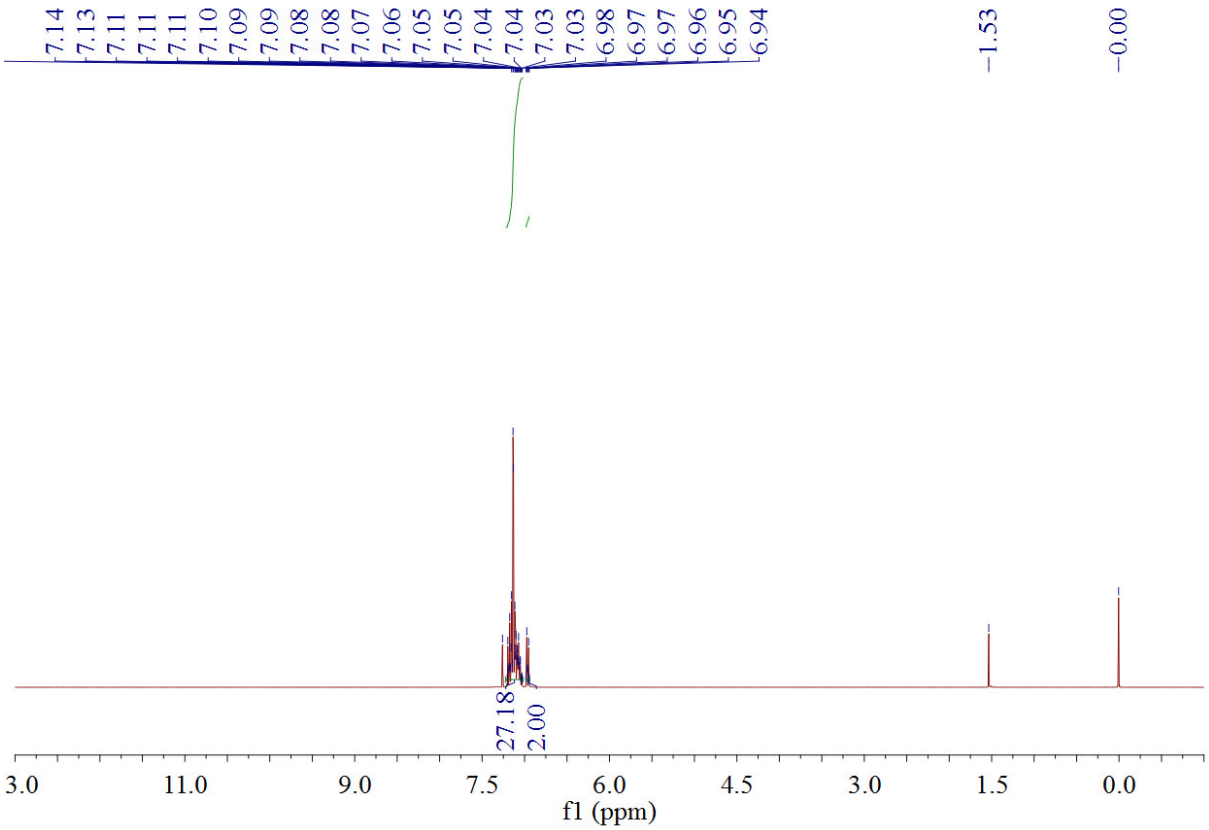

Fig. S22 ^{1}H NMR spectrum of **HPM-Br** in $CDCl_3$.

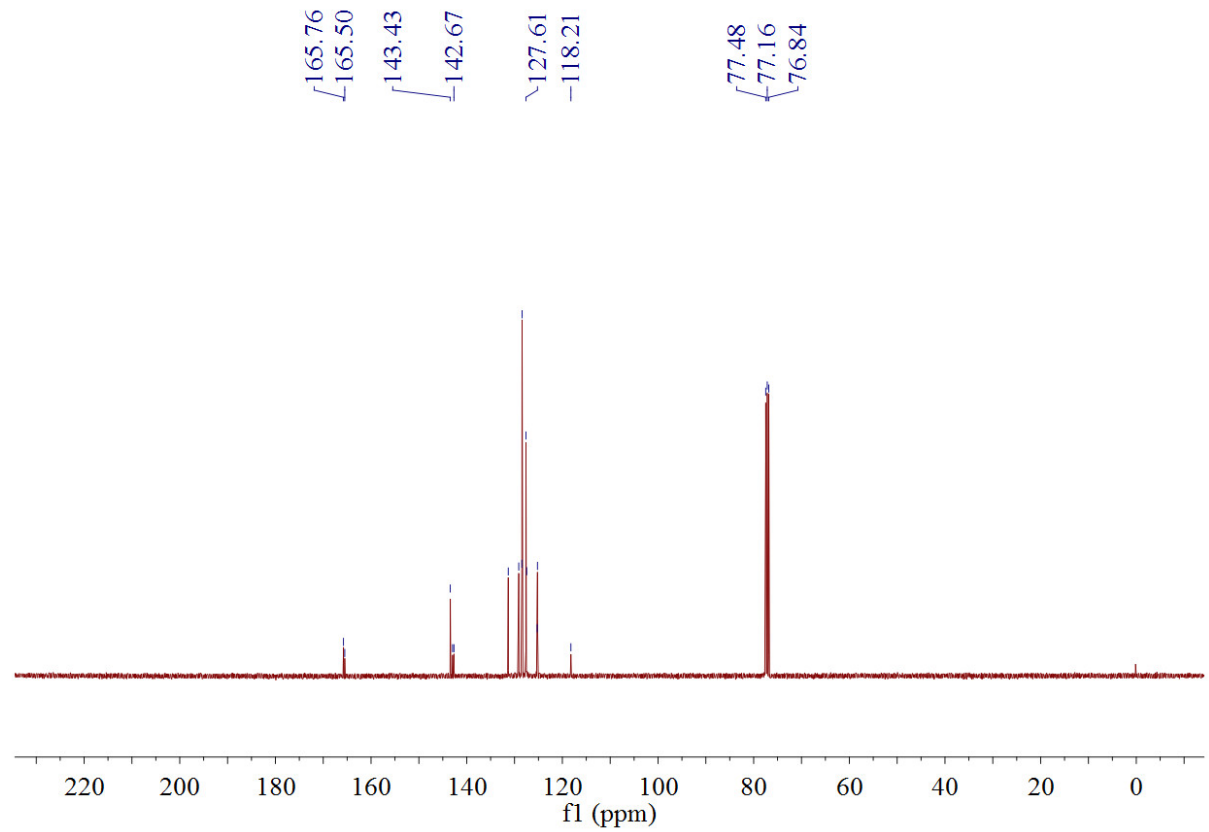

Fig. S23 ^{13}C NMR spectrum of **HPM-Br** in $CDCl_3$.

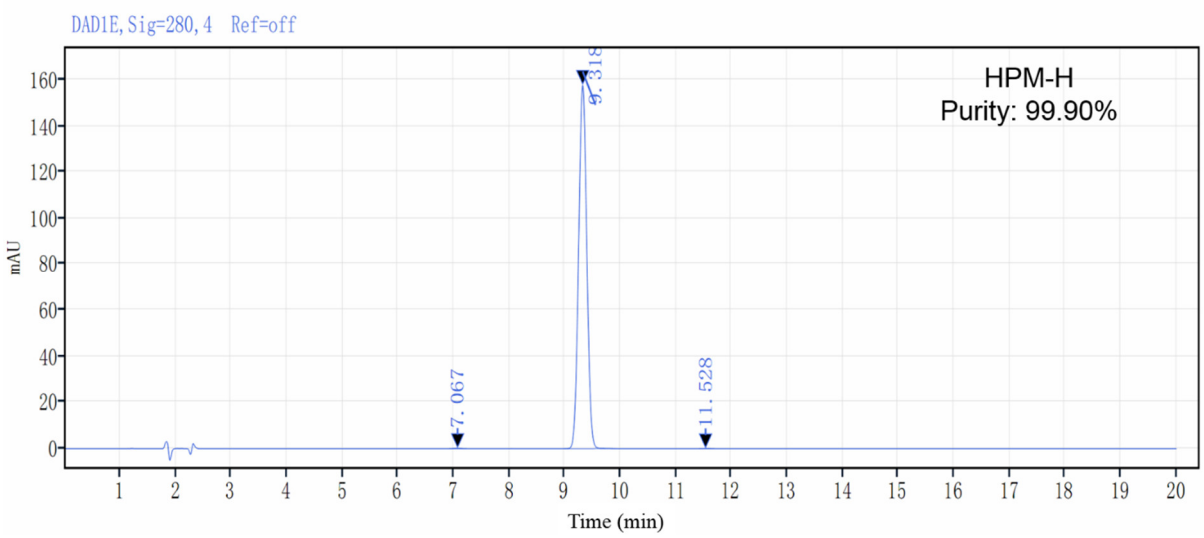

Fig. S24 Purity of **HPM-H** determined by HPLC.

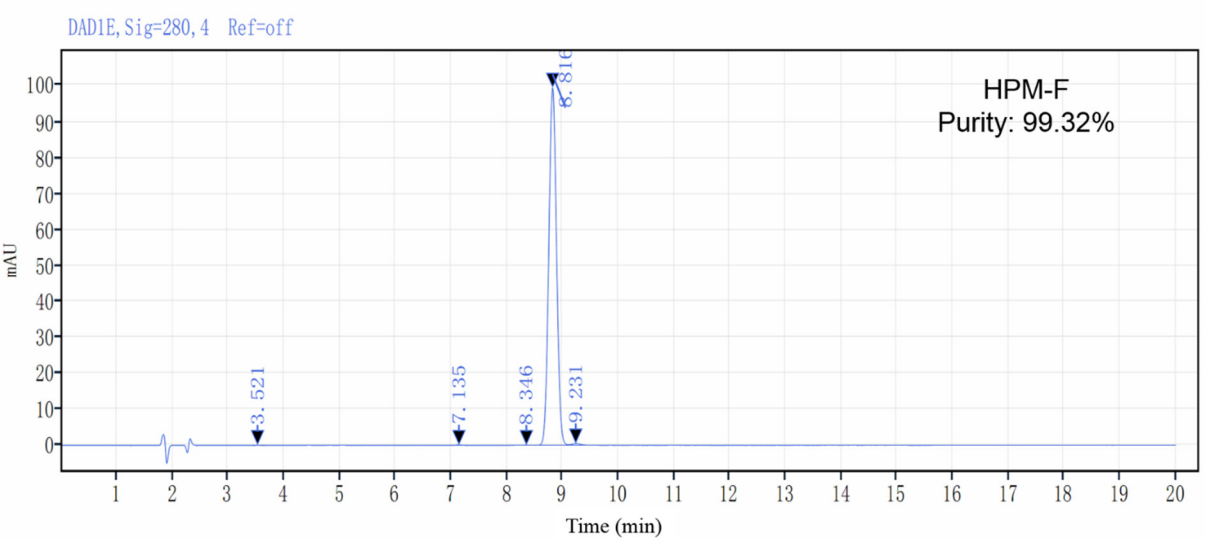

Fig. S25 Purity of **HPM-F** determined by HPLC.

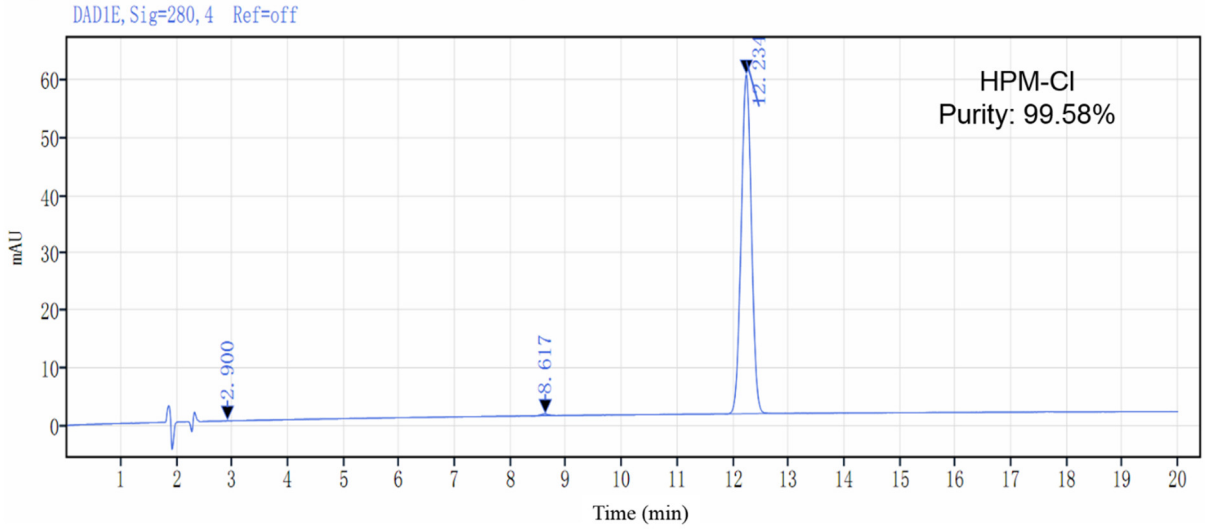

Fig. S26 Purity of **HPM-Cl** determined by HPLC.

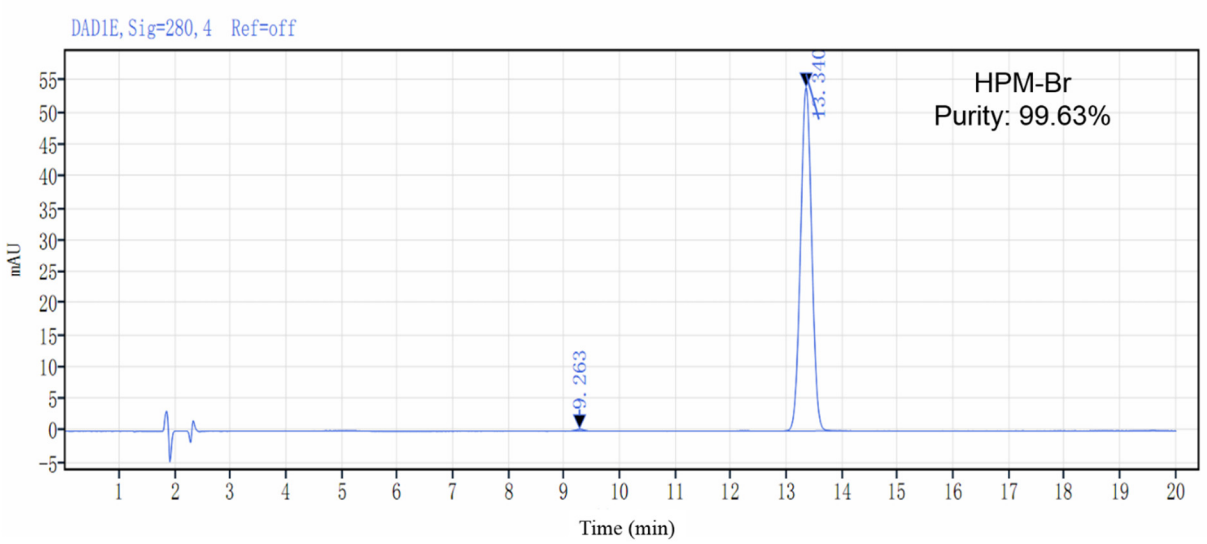

Fig. S27 Purity of **HPM-Br** determined by HPLC.